

Supporting Information for Changing Duration and Spatial Extent of Midlatitude Precipitation Extremes Across Different Climates

J. G. Dwyer,¹, P. A. O’Gorman¹

Contents of this file

Text S1–S3 and Figures S1–S9

Introduction

This document provides supporting text and figures for the main article.

1. Text S1 and Figures S1–S3 describe the CMIP5 results for extended summer seasons.
2. Figure S4 shows the CMIP5 results for extended winter seasons for a lower intensity threshold of the 99th percentile.
3. Figures S5 shows results for the CMIP5 simulations versus latitude.

Corresponding author: J. G. Dwyer, Department of Earth, Atmosphere and Planetary Sciences, Massachusetts Institute of Technology, Cambridge, MA. (jgdwyer@gmail.com)

¹Department of Earth, Atmosphere and Planetary Sciences, Massachusetts Institute of Technology, Cambridge, MA.

4. Text S2 and Figure S6 describe observational results based on CMORPH precipitation data and ERA-interim zonal winds for the extended summer seasons. Figure S7 shows CMIP5 results to compare with Figure S6.

5. Figure S8 shows results for the idealized GCM simulations versus latitude.

6. Text S3 and Figure S9 give results for the idealized GCM simulations in which the advective time scale is based on the eddy phase speed rather than the mean zonal wind.

Text S1: CMIP5 extended summer seasons

We describe the duration and zonal length in CMIP5 for the extended summer seasons which are defined as MJJAS in the NH and NDJFM in the SH. For the control climate, Figure S1 shows that the duration and advective time scale have a similar spatial pattern, and Figure S2a shows that there is a relationship across models between duration and advective time scale. Figure S2b shows that the climate-change response is a reduction in duration in most models: the multimodel mean reduction in duration is $0.7\%K^{-1}$ as compared to a $6.1\%K^{-1}$ increase in intensity. Figure S3 shows that for the (lower) 99th percentile intensity threshold, the relationship with the advective time holds for the control climate and there is a projected reduction in duration in most models, but that the relationship between advective time scale and duration does not hold for the projected changes. This is in contrast to the 99th percentile intensity threshold in the extended winter seasons, for which the relationship between duration and advective time scale holds for both the control climate and the projected changes as shown in Figure S4.

Text S2: CMORPH observational estimates

We calculate observational estimates of the duration and zonal length from the CMORPH precipitation dataset [Joyce et al, 2004]. This dataset provides high-temporal resolution and spatially complete precipitation estimates by propagating and morphing passive microwave precipitation retrievals using geostationary infrared imagery. We use the bias-corrected CRT version of the dataset which is available over the period 1998-2015. We start with the 3-hourly data at 0.25 degree spatial resolution, and we regrid it using spatial averaging to a 2 degree grid which is more comparable to the grids in

the CMIP5 climate models. We present results for latitudes 30° – 60° because CMORPH does not extend poleward of 60° latitude. We calculate the advective time scale using the mean zonal winds from the ERA-interim reanalysis over the same time period and using the same value of $U_0 = 5 \text{ m s}^{-1}$ as for the model analyses.

Figure S6 shows the results for the duration, advective time scale, zonal wind, and zonal length for the extended summer seasons and for the 99th percentile intensity threshold. We consider the extended summer seasons because the CMORPH estimates in midlatitudes have been found to agree better with rain-gauge data in summer than winter, at least over land [e.g., Guo et al 2015]. We use the 99th percentile intensity threshold rather than the 99.9th percentile that was used for the CMIP5 models because a shorter time period is available for CMORPH and because the multimodel mean helped to reduce noise for the model results. The spatial distributions and magnitudes of the duration and advective time scale are similar in some but not all aspects. In particular, the advective time scale captures the tendency for longer durations at lower latitudes.

To facilitate comparison with the CMORPH results in Figure S6, results are presented in Figure S7 for the CMIP5 models for the 99th percentile intensity threshold, extended summer seasons, and the same latitude range as for CMORPH. Spatially averaged over the latitude ranges shown in Figure S6, the duration is 12.2 hours for CMORPH as apposed to the multimodel mean of 14.5 hours and model range of 10.4–20.8 hours for CMIP5.

Text S3: Eddy phase speeds in the idealized GCM simulations

According to Kidston et al. [2011], an increase in the eddy length leads to an increase in eddies' intrinsic westward phase speed relative to the zonal wind. We investigate whether

this effect could be important for the duration of precipitation extremes by calculating an alternative advective time scale based on the eddy phase speed rather than the mean zonal wind. We first calculate the spectrum of the eddy meridional velocity at $\sigma = 0.6$ with respect to zonal phase speed following the approach of Randel and Held [1991]. We then calculate a characteristic eddy phase speed at each latitude as the average phase speed weighted by the spectrum. Figure S9 shows that this eddy phase speed (measured relative to the lower boundary rather than relative to the zonal wind) increases with increasing Δ_T , albeit at a reduced rate compared to the zonal wind, and that the advective time scale still maintains the $\Delta_T^{-1/2}$ scaling when it is calculated using the eddy phase speed.

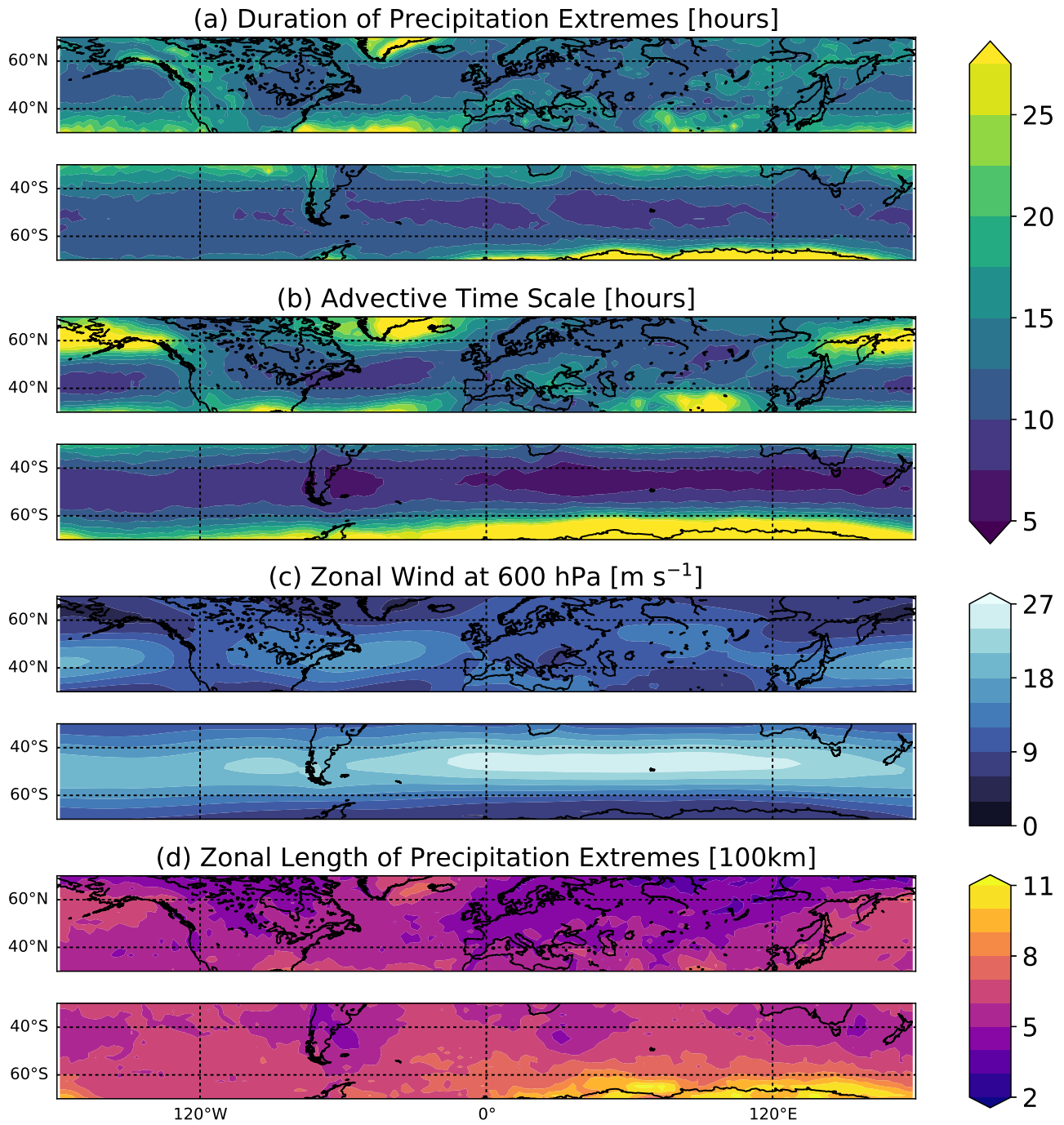


Figure S1. As in Figure 2 for the CMIP5 models, but for the extended summer seasons.

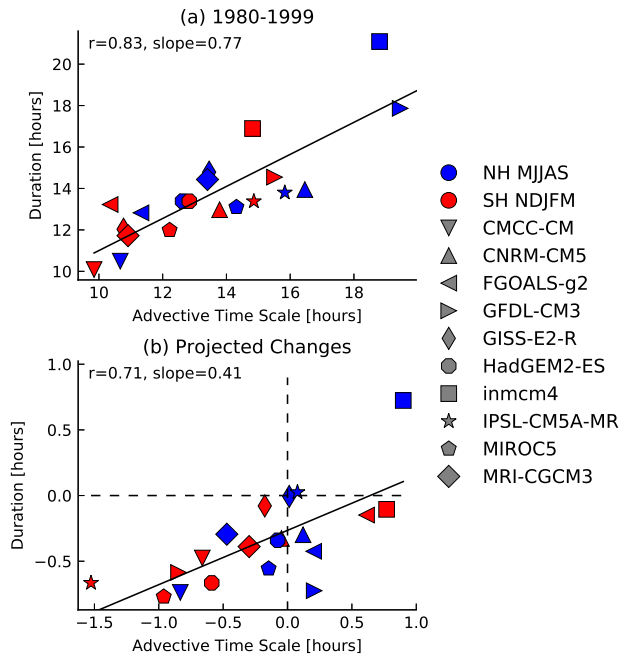


Figure S2. As in Figure 3 for the CMIP5 models, but for the extended summer seasons.

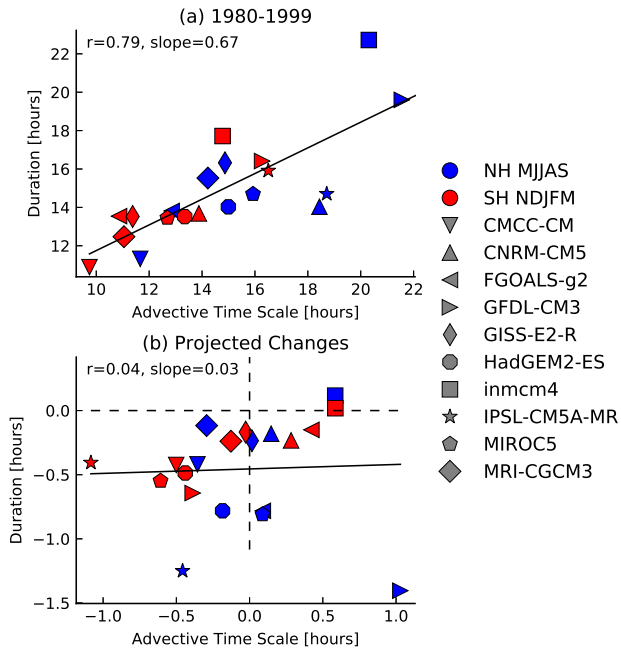


Figure S3. As in Figure 3 for the CMIP5 models, but for the extended summer seasons and I at the 99th percentile. The correlation in b is not significantly different from 0 at the 95% confidence level according to a two-tailed t-test. (All other correlations in the paper are significantly different from zero at this level).

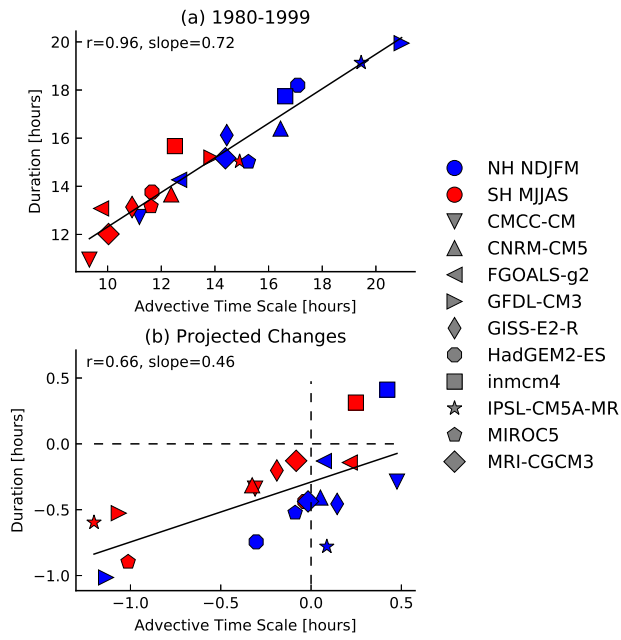


Figure S4. As in Figure 3 for the CMIP5 models, but for I at the 99th percentile.

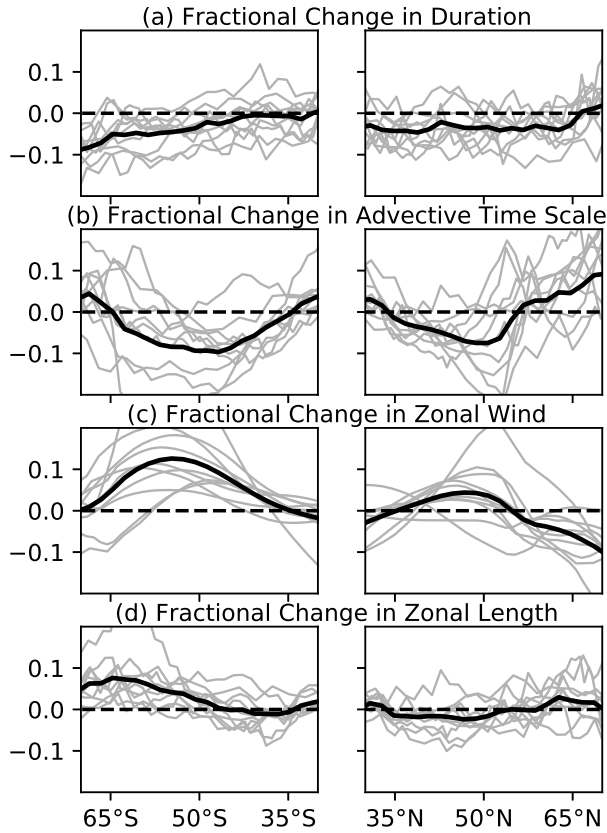


Figure S5. Fractional changes versus latitude for CMIP5 models between the RCP8.5 simulations (2080–2099) and the historical simulations (1980–1999): (a) duration of precipitation extremes, (b) advective time scale, (c) absolute value of the time-mean zonal wind at 600 hPa, and (d) zonal length. The solid black line is the multi-model mean and gray lines are individual models. Each quantity is zonally averaged prior to calculating fractional changes. The results are shown for the default case of extended winter and I at the 99.9th percentile.

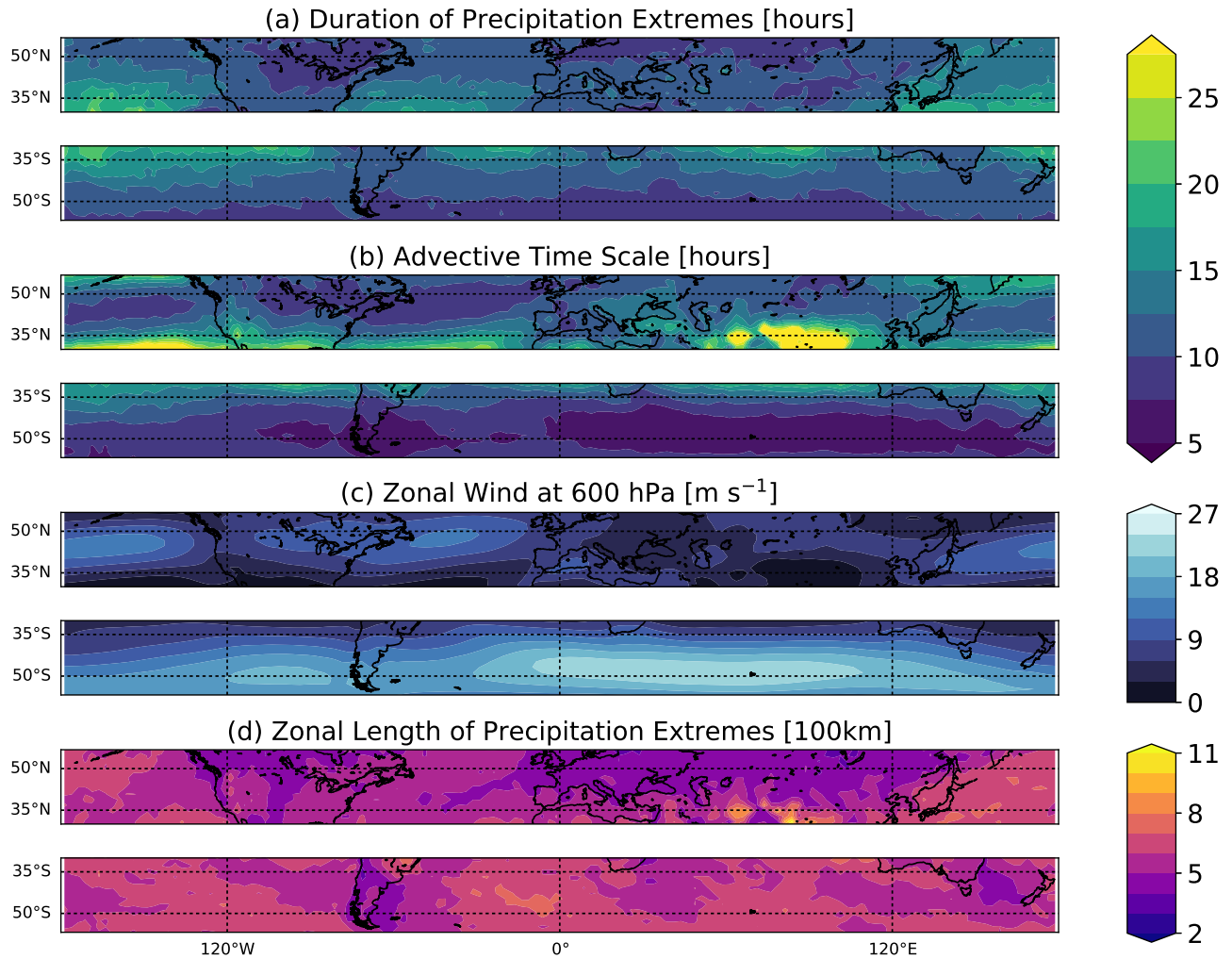


Figure S6. As in Figure 2, but for satellite-measured precipitation from CMORPH over 1998–2015 for the extended summer seasons and using the 99th percentile intensity threshold. CMORPH data is limited to latitudes equatorward of 60° . The advective time scale (b) and zonal wind (c) are calculated using the ERA-Interim reanalysis winds. This figure may be compared with corresponding CMIP5 results in Figure S7.

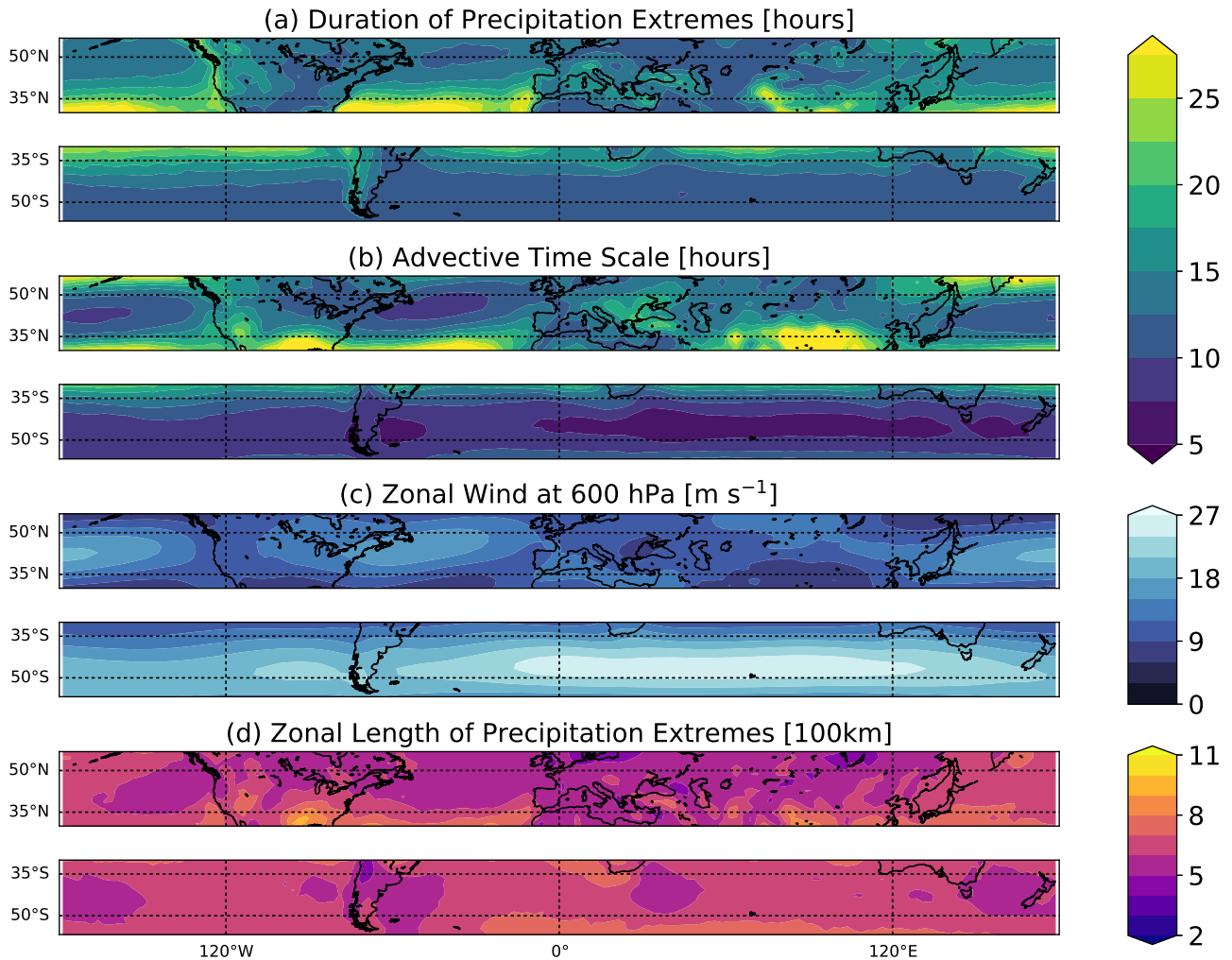


Figure S7. As in Figure 2 for the CMIP5 simulations, but for the extended summer seasons, using the 99th percentile intensity threshold, and only showing latitudes equatorward of 60°. This figure may be directly compared with corresponding CMORPH results in Figure S6.

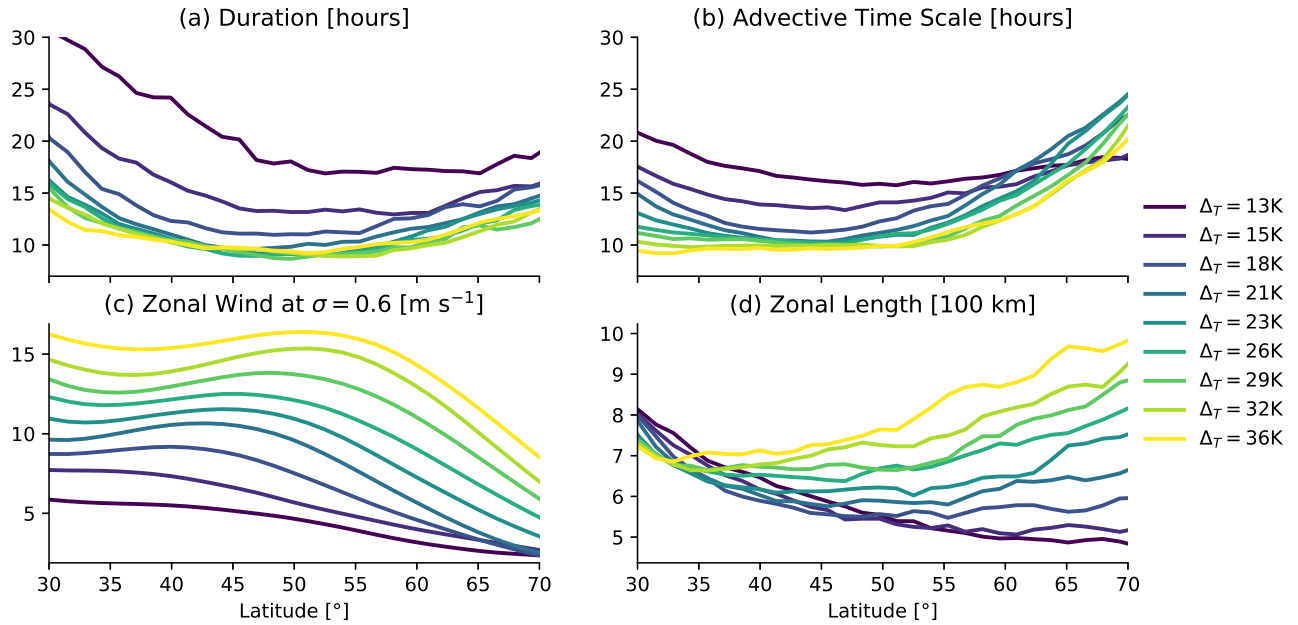


Figure S8. Results versus latitude from the idealized GCM simulations with varying meridional temperature gradients for (a) the duration of precipitation extremes, (b) the advective time scale, (c) the mean zonal wind at $\sigma=0.6$, and (d) the zonal length of extremes.

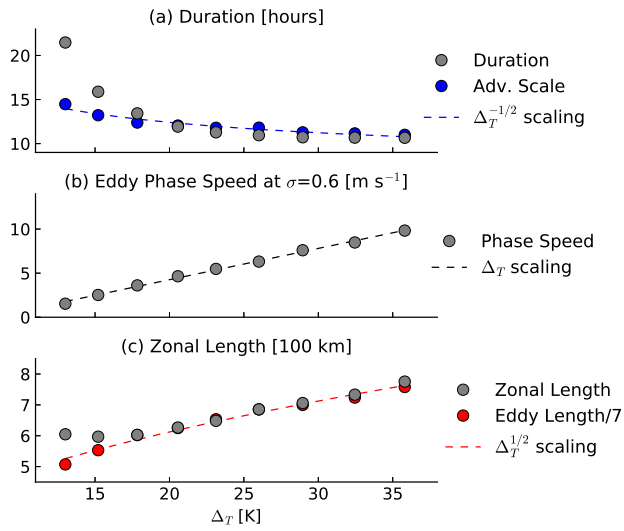


Figure S9. As in Figure 4, but the advective time scale in (a) is calculated with the eddy phase speed and $U_0 = 10 \text{ m s}^{-1}$, and (b) shows the eddy phase speed rather than mean zonal wind.